available at www.sciencedirect.com

ScienceDirect

www.elsevier.com/locate/brainres

BRAIN RESEARCH

Research Report

Expression of chondroitin sulfate proteoglycans in barrel field of mouse and rat somatosensory cortex

Michiru Nakamura[a], *Keiko Nakano*[a], *Shoko Morita*[a], *Toshihiro Nakashima*[a], *Atsuhiko Oohira*[b], *Seiji Miyata*[a,*]

[a]*Department of Applied Biology, Kyoto Institute of Technology, Matsugasaki, Sakyo-ku, Kyoto 606-8585, Japan*
[b]*Department of Perinatology and Neuroglycoscience, Institute for Developmental Research, Aichi Human Service Center, Kasugai, Aichi 480-0392, Japan*

ARTICLE INFO

Article history:
Accepted 4 November 2008
Available online 18 November 2008

Keywords:
Extracellular matrix
Glycosaminoglycan
Barrel
Critical period
Sensory deprivation,
Perineuronal nets
Chondroitin sulfate
Proteoglycan

ABSTRACT

Chondroitin sulfate proteoglycans (CSPGs) consist of chondroitin sulfate (CS) glycosaminoglycans (GAGs) and core protein and regulate the migration, axonal outgrowth, and synaptogenesis in mammalian brains. In the present study, we investigated the localization of CSPGs, the effects of sensory deprivation on the density of perineuronal nets (PNNs), and the effects of chondroitinase ABC (Chase) on the formation of barrel structures in the posterior medial barrel subfield (PMBSF). In developing mouse and rat brains, the immunoreactivity of chondroitin-6-sulfate containing proteoglycan (CS-6-PG), phosphacan, and neurocan was stronger at barrel septa as compared with barrel hollows and surrounding cortex, while the labeling of *Wisteria floribunda* agglutinin (WFA) was observed at barrel hollows. In adult brains, CS-6-PG-immunoreactive and WFA-labeled PNNs were observed mainly at barrel hollows of mouse, but they were seen chiefly at barrel septa of rats. Sensory deprivation of facial vibrissae reduced the number of WFA-labeled PNNs at barrel hollows but not at barrel septa. Intracerebral injection of Chase did not affect the formation of barrel structures in the PMBSF. These data indicate species-dependent heterogeneity of CSPG expression and activity-dependent formation of PNNs in the PMBSF, but CS GAGs have no crucial function in constructing the barrel structures during early postnatal development.

1. Introduction

The rodent somatosensory system is an excellent model to study neuronal pattern formation and neuronal plasticity (Fox, 1992; Frostig, 2006; for review, see Peterson, 2007). In the primary somatosensory cortex, periphery-related patterns of sensory receptors are recapitulated in layer IV as an array of multineuronal structures called “barrels” (Woolsey and Van der Loos, 1970). In barrels, neurons are arranged in cylindrical or oval-shaped rings that are separated from

* *Corresponding author*. Fax: +81 75 724 7796.
E-mail address: smiyata@kit.ac.jp (S. Miyata).

Abbreviations: Chase, chondroitinase ABC; ConA, concanavalin A; CO, cytochrome oxidase; CS, chondroitin sulfate; CSPGs, chondroitin sulfate proteoglycans; CS-6-PG, chondroitin-6-sulfate containing proteoglycan; ECM, extracellular matrix molecules; GAG, glycosaminoglycan; GFAP, glial fibrillar acidic protein; NeuN, neuron-specific nuclear antigen; PMBSF, posterior medial barrel subfield; PN, postnatal day; PNNs, perineuronal nets; PNA, peanut agglutinin; VVA, *Vicia villosa* agglutinin; WFA, *Wisteria floribunda* agglutinin; WGA, wheat germ agglutinin

0006-8993/$ – see front matter © 2008 Elsevier B.V. All rights reserved.
doi:10.1016/j.brainres.2008.11.022

neighbors by hypocellular "septa". Those cell-dense walls surround cell-sparse "hollows" containing thalamocortical afferent terminals (Woolsey and Van der Loos, 1970). The removal of sensory information by whisker follicle cauterization or denervation induces a disorganization of structural barrel pattern. These barrel structures are consolidated during the first few days (critical period) through somatosensory inputs from whiskers, so that the removal of sensory information has little effect upon the organization of barrel structures over postnatal day 5 (PN5) (Van der Loos and Woolsey, 1973; Woolsey and Wann, 1976; Wong-Riley and Welt, 1980; Schlaggar et al., 1993). The organization of barrel structures is primarily determined by a genetic program such as FGF-8 as well as the general patterning of the neocortex (Fukuichi-Shimogori and Grove, 2001). Moreover, refinement of barrel structures is likely to be guided by activity-dependent mechanisms, since barrel structures are less clearly defined or absent in mice with genetic knockout of several genes such as NMDA receptor (Iwasato et al., 2000), phospholipase C β1 (Hannan et al., 2001), adenyl cyclase 1 (Welker et al., 1996), and monoamine oxidase A (Cases et al., 1996).

The extracellular matrix (ECM) molecules are involved in cell–substrate interactions during morphogenesis of the nervous system in developing brains and plastic modifications of neuronal connectivity in adult brains. Chondroitin sulfate proteoglycans (CSPGs) have been recognized as important constituents of the brain's ECM and are considered to participate in neural network formation (for reviews, see Bovolenta and Fernaud-Espinosa, 2000; Galtrey and Fawcett, 2007). CSPGs consist of a core protein and sulfated glycosaminoglycans (GAGs) (Bandtlow and Zimmermann, 2000; Yamaguchi, 2000) and are generally known to inhibit neurite outgrowth (Oohira et al., 1991; Katoh-Senba et al., 1995). Moreover, recent studies have shown that CSPGs are responsible for structural plasticity in adult brains such as functional recovery after spinal cord injury (Bradbury et al., 2002), axonal sprouting of cerebellar Purkinje neurons (Corvett and Rossi, 2005), and reactivation of ocular dominance plasticity in the visual cortex (Pizzorusso et al., 2002, 2006).

Perineuronal nets (PNNs) are a specialized form of ECM that appears at the end of the critical period (Celio et al., 1998). PNNs have been visualized using a variety of methods including the labeling of lectins such as *Wisteria floribunda* agglutinin (WFA) and *Vicia villosa* agglutinin (VVA) that have high affinities to *N*-acetylgalactosamine (Härtig et al., 1992; Brückner et al., 1993), the binding of hyaluronic acid binding protein to hyaluronic acid (Brückner et al., 1998, 2000), and immunological staining for CSPGs (Brückner et al., 1998, 2000). PNNs are frequently seen around parvalbumin-immunoreactive GABAergic interneurons in the cerebral cortex (Brückner et al., 1994; Brückner and Grosche, 2001). During postnatal development, PNNs are first detected at the onset of the period during which the pattern of neuronal activity determines the mature synaptic circuitry and neuronal phenotype in the visual cortex (Köppe et al., 1997; Brückner et al., 2000). It is also shown that dark-rearing from birth prolongs the duration of the critical period and attenuates the expression of several CSPGs (Lander et al., 1997; Pizzorusso et al., 2002). PNNs are well preserved and maintained for 3–10 weeks in slice culture, indicating that the differentiation of PNNs is part of the developmental program maintained in brain tissue *in vitro* (Brückner and Grosche, 2001). It is also shown that the formation of PNNs in brain slice culture is promoted via calcium signaling (Brückner and Grosche, 2001). More recently, we have demonstrated that neurons themselves are able to construct a PNNs structure in dissociated cortical culture without glial cells (Miyata et al., 2005, 2007), and later this was confirmed in hippocampal neuron culture (John et al., 2006).

Various ECM molecules are shown to be expressed specifically in the somatosensory barrel cortex. Lectin histochemistry has revealed that lectin binding is absent from barrel hollows in the early postnatal period using peanut agglutinin (PNA), concanavalin A (ConA), and wheat germ agglutinin (WGA) (Cooper and Steindler, 1986; Steindler et al., 1995). It has been demonstrated that CSPGs such as neurocan and DSD-1-PG are also absent from barrel hollows in the early developing brains (Watanabe et al., 1995; Steindler et al., 1995). Tenascin-C, which is able to interact with CSPGs, is shown to be expressed predominantly at barrel septa, but tenascin-C-deficient mice show normal distribution of DSD-1-PG immunoreactivity and PNA labeling (Steindler et al., 1995; Mitrovic et al., 1996; Cybulska-Klosowicz et al., 2004). A recent study has shown that trimming of facial vibrissae attenuates the expression of Cat-315-immunoreactive aggrecan without changing the number of WFA-labeled PNNs (McRae et al., 2007). Moreover, the deprivation of sensory information from facial vibrissae decreases the number of VVA-labeled PNNs in the PMBSF (Bahia et al., 2008).

At present, however, the functional significance of CSPGs in pattern formation of barrel structures is not completely understood. In the present study, therefore, we examined the spatiotemporal expression of CS GAGs and major CSPGs such as phosphacan and neurocan in the PMBSF of the somatosensory cortex using rats and mice to show the heterogeneity of CSPG expression. Furthermore, we investigated the effects of sensory deprivation of facial vibrissae on

Fig. 1 – Tangential sections showing the histochemical staining of CO and red-fluorescence Nissl and the immunohistochemical staining of NeuN and GFAP in the PMBSF of the somatosenosry cortex using mice and rats. (A–D) In PN10 and adult mice, barrel structures were clearly observed by CO and Nissl stainings and NeuN immunostaining at low magnification view and each barrel hollow was seen clearly by double labeling of Nissl staining and NeuN immunostaining at high magnification view. (E–E″) In rats, barrel structures were clearly observed by CO staining, but each barrel hollow was not clearly seen by NeuN immunostaining and Nissl staining. (F–K′) The immunohistochemistry revealed that aggregates (arrowheads) of GFAP-positive astrocytes distributed in the PMBSF of mice and rats in spite of uniform distribution of them at surrounding cortex (nonbarrel cortex). Scale bars = A and C (500 μm), B, D, and E–K (100 μm).

the density of WFA-labeled PNNs and the effects of chondroitinase ABC (Chase) injection on the formation of barrel structures in the PMBSF. Here, we showed that the expression of CSPGs was observed concomitantly with structural barrel formation and the construction of CSPG-containing PNNs depends on sensory information. Moreover, CS GAGs did not have any crucial role in controlling the formation of barrel structures.

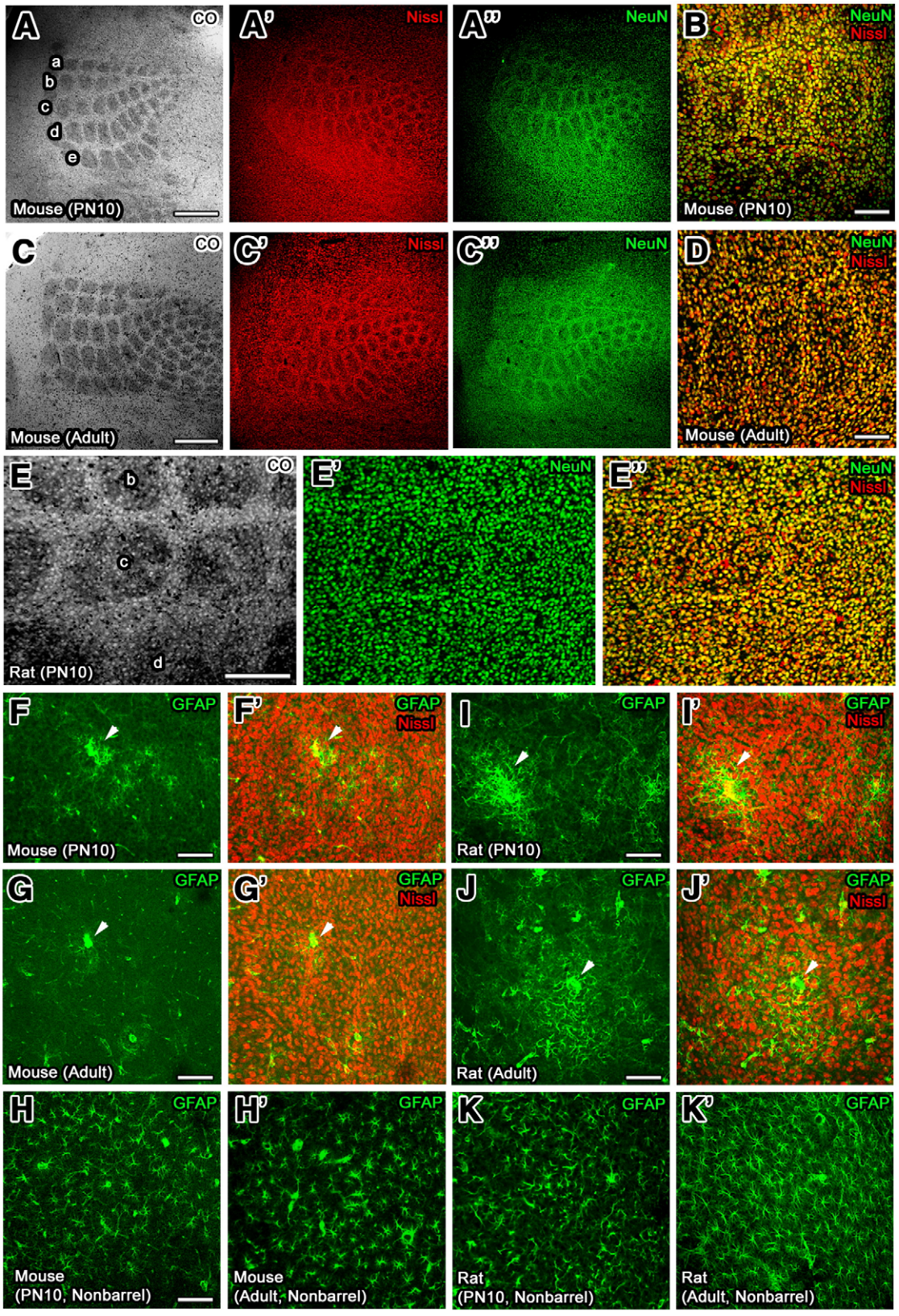

2. Results

2.1. *Comparison of PMBSF structures in mouse and rat*

The PMBSF is a subfield of the rodent primary somatosensory cortex that represents 5 rows of large whiskers with exquisite order. In the PMBSF of PN10 and adult mice, a typical barrel structure was clearly visible by staining presynaptic terminals of thalamic afferent nerves with cytochrome oxidase (CO) histochemistry (Figs. 1A and C) and by labeling postsynaptic neurons with both red-fluorescence Nissl staining (Figs. 1A′ and C′) and neuron-specific nuclear antigen (NeuN) immunostaining (Figs. 1A″ and C″). Higher magnification showed that each barrel hollow was separated from other barrel hollows by cell-dense walls (Figs. 1B and D). In contrast to mice, in rats hollows were revealed by either Nissl staining or NeuN immunostaining (Figs. 1E′ and E″), although a typical barrel structure was observed with CO staining (Fig. 1E). Some of CSPGs are known to be produced by glial cells (for review,

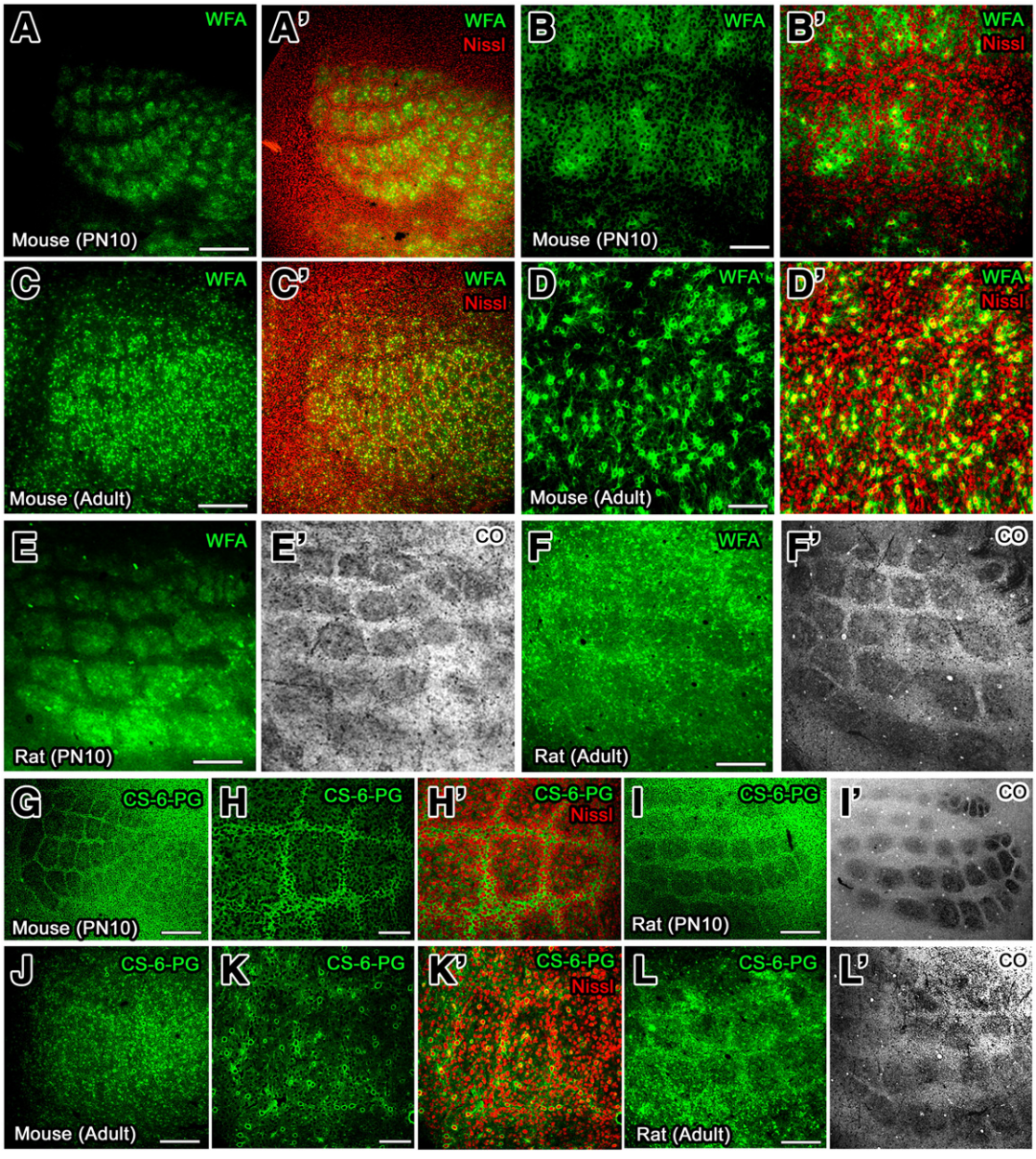

Fig. 2 – Tangential sections showing the localization of WFA labeling and CS-6-PG-immunoreactivity in the PMBSF of mice and rats. (A–D′) In PN10 mice, WFA labeling was seen at barrel hollows in the PMBSF to show vibrissa-related pattern. In adult animals, more WFA-labeled PNNs were observed at barrels in the PMBSF as compared with surrounding cortex. (E–F′) Stronger WFA labeling was observed at barrel hollows in the PMBSF of PN10 rats and more WFA-labeled PNNs were seen at barrel septa as compared with barrel hollows in adult rats. (G–L′) The immunoreactivity of CS-6-PG was observed at barrel septa of the PMBSF in PN10 mice and rats. CS-6-PG-immunoreactive PNNs were seen at barrel hollows in adult mice and at barrel septa in adult rats. Scale bars = A, C, E, F, G, I, J, and L (500 μm), B, D, H, and K (100 μm).

see Celio and Blumcke, 1994; Celio et al., 1998), and therefore we examined the localization of GFAP-positive astrocytes in the PMBSF of mice and rats (Figs. 1F–K′). While GFAP-positive astrocytes formed large aggregates in the PMBSF of mice and rats, they were distributed uniformly in the surrounding cortex (nonbarrel regions).

2.2. *Spatiotemporal expression of CSPGs in PMBSF*

To examine the spatiotemporal expression of CSPGs in the PMBSF, we used WFA lectin and the antibody against chondroitin-6-sulfate containing proteoglycan (CS-6-PG) (Fig. 2). It is shown that WFA lectin recognizes N-acetylgalactosamines of CS GAGs (Härtig et al., 1992; Brückner et al., 1993) and anti-CS-6-PG antibody recognizes 6-sulfated stubs of core proteins disclosed after Chase treatment (Miyata et al., 2005). Stronger WFA labeling was observed at barrel hollows as compared with barrel septa and surrounding cortex in PN10 mice (Figs. 2A, A′, B, and B′). More WFA-labeled PNNs were seen at barrel hollows as compared with barrel septa and surrounding cortex in adult mice (Figs. 2C, C′, D, and D′). In PN10 rats, similar to mice, stronger WFA labeling was observed at barrel hollows as compared with barrel septa and surrounding cortex (Figs. 2E and E′), and more WFA-labeled PNNs were seen at barrel septa as compared with barrel hollows and surrounding cortex (Figs. 2F and F′). The immunoreactivity of CS-6-PG was weaker at barrel hollows as compared with barrel septa and surrounding cortex in PN10 mice and rats (Figs. 2G, H, H′, I, and I′). In adult mice, more CS-6-PG-immunoreactive PNNs were observed at both barrel hollows and septa as compared with surrounding cortex (Figs. 2J, K, and K′). In contrast to mice, more CS-6-PG-immunoreactive PNNs were seen at barrel septa of adult rats as compared with barrel hollows and surrounding cortex (Figs. 2L, and L′). CS-6-PG immunohistochemistry and WFA labeling histochemistry revealed that spatial expression of CSPGs in PN5 mice and rats were the same to that seen in PN10 animals.

2.3. *Spatiotemporal expression of phosphacan and neurocan in PMBSF*

The immunoreactivity of 6B4 phosphacan was weaker at barrel hollows as compared with barrel septa and surrounding cortex in PN10 rodents (Figs. 3A, A′, B, B′, E, E′, F, and F′). In adult animals, more 6B4-phosphacan-immunoreactive PNNs were observed at barrel hollows as compared with barrel septa and surrounding cortex (Figs. 3C, C′, D, D′, G, G′, H, and H′). The immunoreactivity of 3F8 phosphacan was weaker at barrel hollows in the PMBSF as compared with barrel septa and surrounding cortex in PN10 animals (Figs. 3I, J, J′, K and K′), while in adult rodents more 3F8-immunoreactive PNNs were seen at barrel septa as compared with barrel hollows and surrounding cortex (Figs. 3L, M, M′, N, and N′). These results indicate the heterogeneous phosphacan composition of PNNs in the PMBSF. In PN10 rats, the immunoreactivity of 1G2 and PAb291 neurocan was weaker at barrel hollows as compared with barrel septa and surrounding cortex (Figs. 3O, O′, P, and P′), whereas the their immunoreactivity did not delineate the PMBSF of the PN10 and adult mice (data not shown). WFA-labeled PNNs were often seen at parvalbumin-immunoreactive neurons which are considered as GABAergic neurons in the PMBSF of mice (Figs. 4A, A′, A″, and A″) and rats (Figs. 4C, C′, C″, and C″) and WFA-labeled PNNs were frequently seen to contain 6B4 immunoreactivity (Figs. 4B, B′, B″, B″, D, D′, D″ and D″). These results indicate that PNN-containing neurons in the PMBSF are GABAergic neurons.

2.4. *Effect of sensory deprivation on number of PNNs and Chase treatment on formation of barrel structures*

In order to assess whether sensory information from facial vibrissae affects the formation of PNNs, facial vibrissae were removed on PN1 and examined the number of WFA-labeled PNNs in rat PMBSF on PN56 (Fig. 5). Sensory deprivation significantly reduced the number of WFA-labeled PNNs in barrel hollows but not in barrel septa. Moreover, to assess whether or not CSPGs participate in controlling the formation of barrel structures, Chase was injected intracerebrally into the somatosensory cortex on PN0, PN2, PN4, and PN6, and we examined the formation of barrel structures in the PMBSF of mice on PN7 (Fig. 6). The quantitative analysis of barrel structures of the PMBSF showed that the percentage of row C and D and D/C ratio were not changed with Chase treatment. This result indicates that the intracerebral injection of Chase did not disturb the formation of barrel structures.

3. Discussion

The CSPGs are now known to be concerned with cell–substrate interactions during brain development and plastic modifications of neuronal connectivity in adult brains. The present study investigated the spatiotemporal expression of CSPGs in the PMBSF of PN10 and adult rodents using lectin histochemistry and immunohistochemistry, and resultant data were summarized in Table 1. The main findings of the present study were as follows; 1) in the early developing brains of PN10 rodents, the expression of CSPGs was observed simultaneously with the appearance of barrel structures. WFA labeling was stronger in barrel hollows, while the immunoreactivity for CS-6-PG, phosphacan, and neurocan were lower in barrel hollows than surrounding cortex. 2) In adult brains, more WFA-labeled and CS-6-PG-immunoreactive PNNs in rats were observed in rat septa than barrel hollows, while those in mice were likely to be seen with greater intensity in barrel hollows, indicating the distinct PNN distribution pattern between mice and rats. 3) In the PMBSF of adult rodents, the distribution pattern of 6B4- and 3F8-phosphacan-immunoreactive PNNs in barrels and septa complemented each other. 4) GFAP-immunoreactive astrocytes constituted large aggregates within the PMBSF, although they were distributed uniformly in the surrounding cortex. 5) The deprivation of facial vibrissae significantly decreased the number of WFA-labeled PNNs in barrel hollows but not barrel septa in rats. 6) Intracerebral injection of Chase did not affect the early formation of barrel structures in the PMBSF of mice.

The barrel cytoarchitecture is different between mice and rats; In rats, large gaps called septa are observed between individual barrels. In mice, however, the gap is not obvious

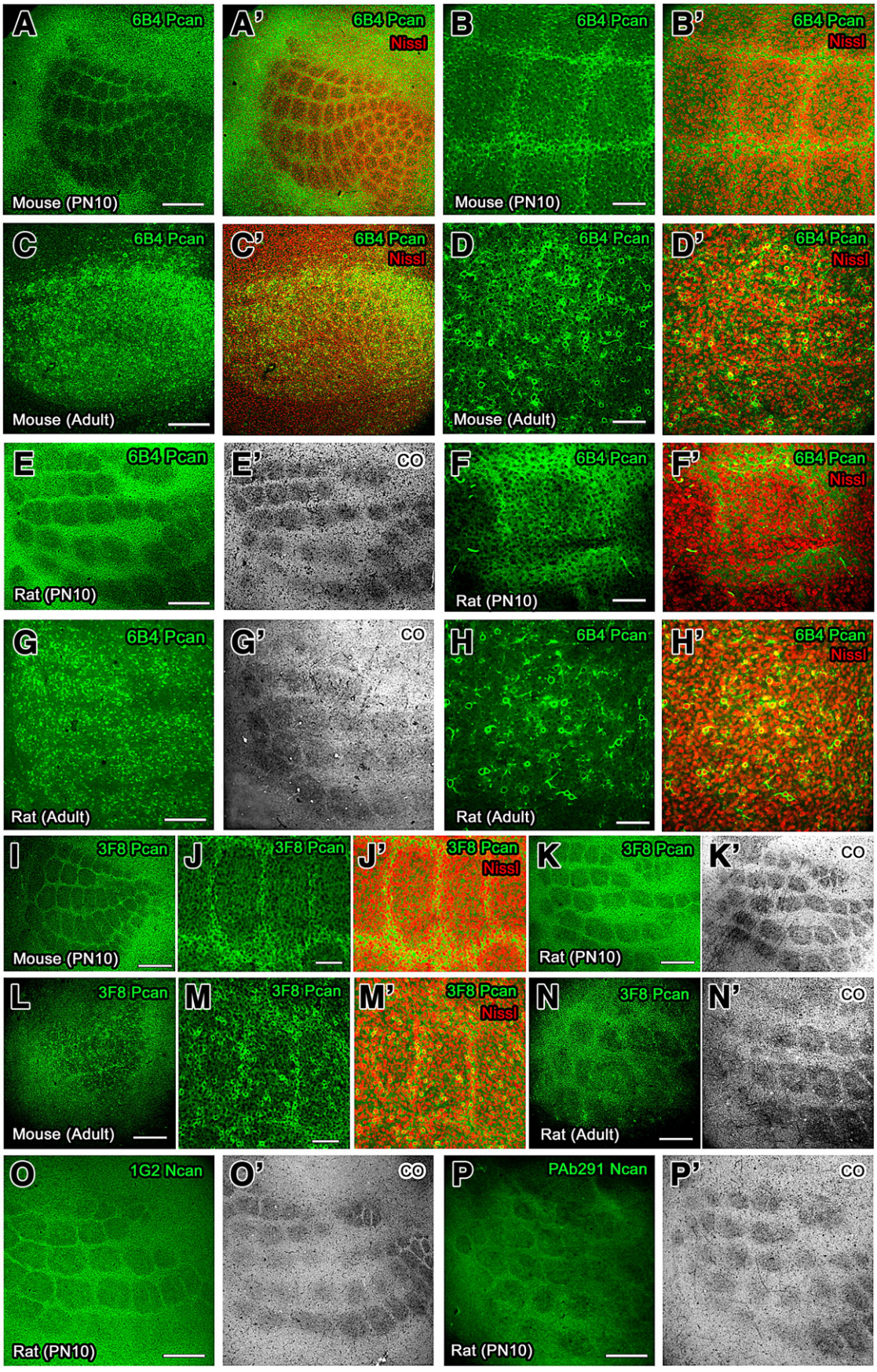
A
6B4 Pcan
Mouse (PN10)
A'
6B4 Pcan
Nissl
B
6B4 Pcan
Mouse (PN10)
B'
6B4 Pcan
Nissl
C
6B4 Pcan
Mouse (Adult)
C'
6B4 Pcan
Nissl
D
6B4 Pcan
Mouse (Adult)
D'
6B4 Pcan
Nissl
E
6B4 Pcan
Rat (PN10)
E'
CO
F
6B4 Pcan
Rat (PN10)
F'
6B4 Pcan
Nissl
G
6B4 Pcan
Rat (Adult)
G'
CO
H
6B4 Pcan
Rat (Adult)
H'
6B4 Pcan
Nissl
I
3F8 Pcan
Mouse (PN10)
J
3F8 Pcan
J'
3F8 Pcan
Nissl
K
3F8 Pcan
Rat (PN10)
K'
CO
L
3F8 Pcan
Mouse (Adult)
M
3F8 Pcan
M'
3F8 Pcan
Nissl
N
3F8 Pcan
Rat (Adult)
N'
CO
O
1G2 Ncan
Rat (PN10)
O'
CO
P
PAb291 Ncan
Rat (PN10)
P'
CO

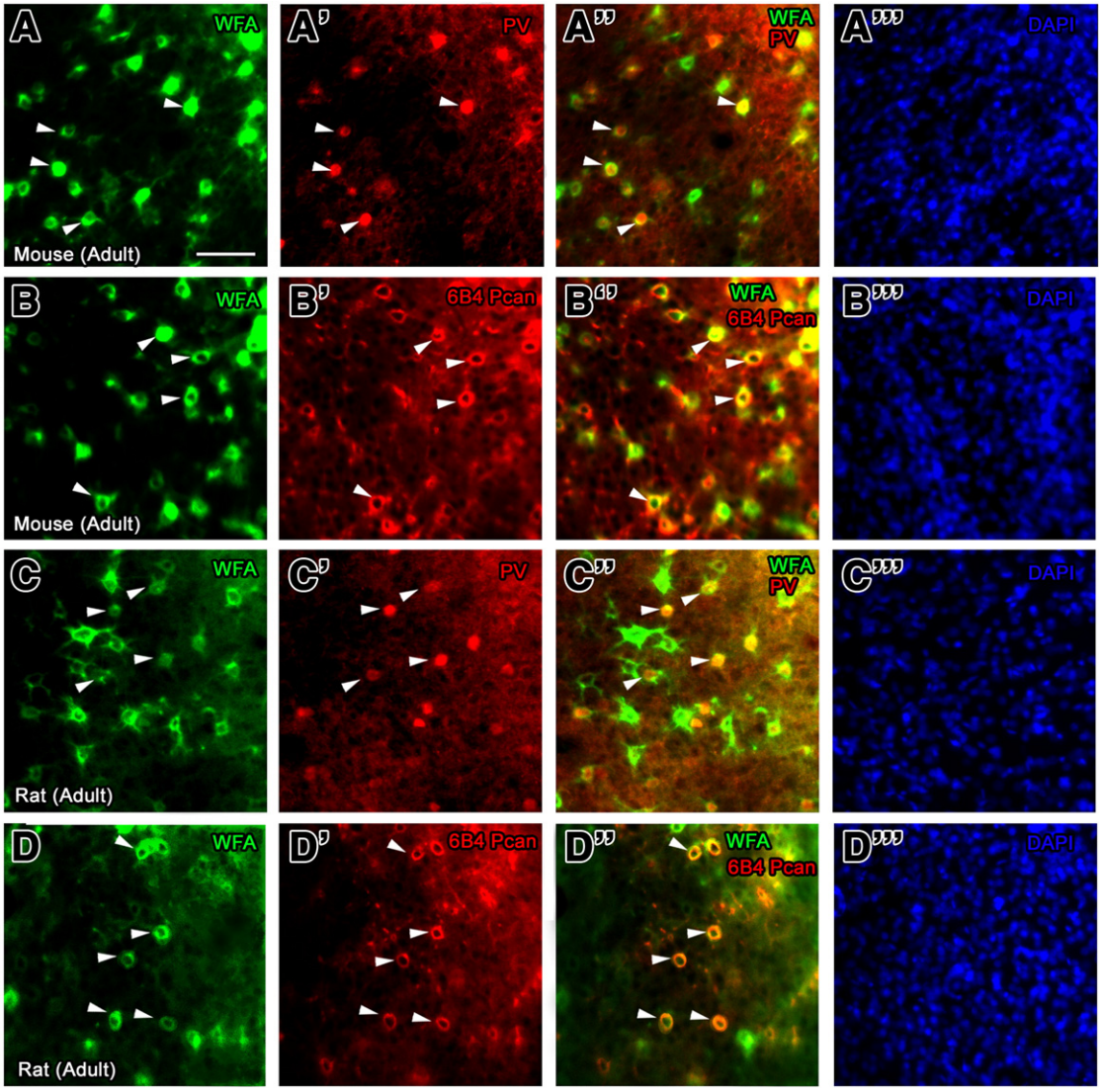

Fig. 4 – Tangential sections showing the colocalization of WFA labeling and the immunoreactivity for 6B4 phosphacan or parvalbumin in the PMBSF of mice and rats. (A–B″) In adult mice, WFA-labeled PNNs were often seen at parvalbumin-positive neurons in the PMBSF and were frequently observed to colocalize with the immunoreactivity of 6B4 phosphacan (arrowheads). (C–D″) In adult rats, WFA-labeled PNNs were often seen at parvalbumin-positive neurons in the PMBSF and were frequently observed to colocalize with the immunoreactivity of 6B4 phosphacan (arrowheads). PV, parvalbumin. Scale bar = 100 μm.

and neighboring barrels are tightly apposed to each other (For review, see Peterson, 2007). In the present study, the mouse PMBSF was clearly observed not only by the visualization of presynaptic terminal (CO staining and GAP-43 immunostaining) but also by the visualization of postsynaptic neurons (Nissl staining and NeuN immunostaining). On the other

Fig. 3 – Tangential sections showing the localization of phosphacan and neurocan in the PMBSF of mice and rats. (A–D′) In PN10 mice, the immunoreactivity of 6B4 phosphacan was eliminated at barrel hollows in the PMBSF to show negative image of vibrissa-related pattern. In adult mice, more 6B4-phosphacan-labeled PNNs were observed at barrel hollows in the PMBSF as compared with barrel septa and surrounding cortex. (E–H′) Spatiotemporal expression of 6B4 phosphacan in rats was similar to that of mice. The immunoreactivity of 6B4 phosphacan was absent in the PMBSF of PN10 rats and more 6B4-phosphacan-labeled PNNs were observed in the PMBSF of adults. (I–N′) The immunoreactivity of 3F8 phosphacan was absent at barrel hollows in the PMBSF to show negative image of vibrissa-related pattern as seen by 6B4 phosphacan. In adult animals, however, more 3F8-phosphacan-labeled PNNs were observed at barrel septa in the PMBSF as compared with barrel hollows and surrounding cortex. (O–P′) The immunoreactivity of 1G2 and PAb291 neurocan was absent at barrel hollows in the PMBSF in PN10 rats. Pcan, phosphacan; Ncan, neurocan. Scale bars = A, C, E, G, I, K, L, N, O, and P (500 μm), B, D, F, H, J, and M (100 μm).

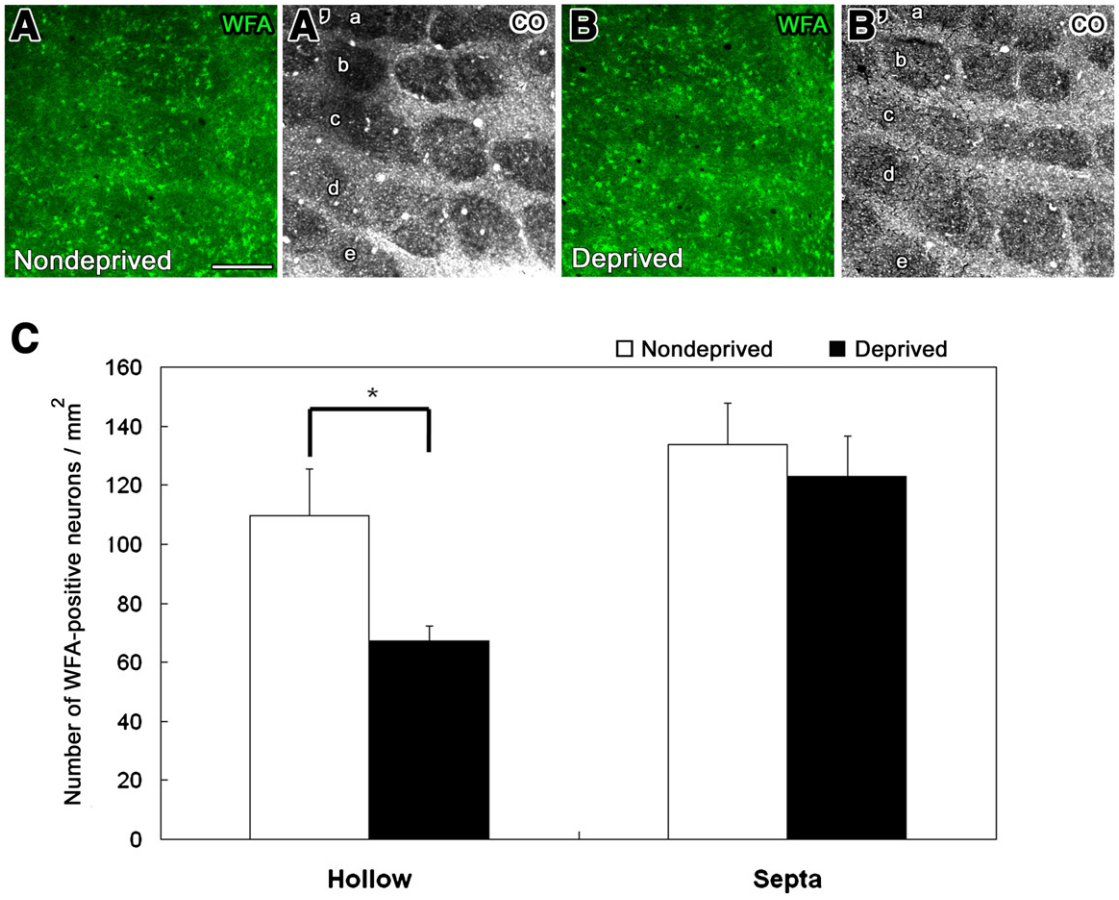

Fig. 5 – Effects of sensory deprivation on the number of WFA-labeled PNNs in the PMBSF of rats. (A–B′) Tangential sections showing WFA-labeled PNNs in a row C barrel of nondeprived and deprived PMBSF. (C) The quantitative analysis revealed that the sensory deprivation of facial vibrissae reduced the number of WFA-positive PNNs in barrel hollows but not in barrel septa. *P<0.05. Scale bar=100 μm.

hand, the rat PMBSF was not clearly visualized with Nissl staining and NeuN immunostaining. In the present study, PNNs were observed mainly inside barrel hollows in mice although they were seen chiefly in barrel septa of rats by using both WFA labeling and CS-6-PG immunohistochemistry. PNNs are known to be formed around GABAergic interneurons (Brückner et al., 1994; Brückner and Grosche, 2001). The immunohistochemistry for glutamic acid decarboxylase reveals that the somata of GABAergic interneurons are located along the sides of the barrel structure in both mice and rats (Lin et al., 1985). Therefore, the dissimilarity of PNNs between mice and rats is possibly due to the different distribution of CSPGs rather than GABAergic interneurons. These results indicate that there is a species-dependent heterogeneity between mouse and rat in basic neuronal arrangement of barrel structures and distribution of PNNs.

The present study further revealed that GFAP-immunoreactive astrocytes constituted large aggregates within the PMBSF in spite of the uniform distribution of GFAP-immunoreactive astrocytes in the surrounding cortex. This observation is essentially different from previous studies; glial glutamate transporter, GLAST and GLT-1 are early and selectively expressed in numerous astrocytes in the PMBSF from PN5 to PN10 (Voutsinos-Porche et al., 2003). The levels of GLAST markedly increase during the most active period of synaptogenesis (Furuta et al., 1997), while the expression of GFAP in astrocytes increases gradually throughout the adult lifespan of mice, rats, and humans (Eng et al., 2000). Taken together, these results indicate that GFAP-immunoreactive astrocytes, possibly mature astrocytes, constitute large aggregates in the PMBSF.

In the PMBSF, lectin labeling such as ConA (specific for N-acetylgalactosamine), PNA (specific for mannose), and WGA (specific for N-acetylglucosamine and N-acetylneuraminic acid) is weaker in barrel hollows than in both septa and the surrounding cortex on early postnatal animals (Cooper and Steindler, 1986; Steindler et al., 1995). Moreover, the expression of CSPGs such as neurocan and DSD-1-PG is weaker in barrel hollows of infant animals (Watanabe et al., 1995; Steindler et al., 1995). In the present study, the immunoreactivity of CS-6-PG, 6B4 and 3F8 phosphacan, and 1G2 and PAb291 neurocan were absent at barrel hollows in early developing brains and this observation coincides with the above previous results. In contrast, the labeling of WFA (specific for N-acetylgalactosamine) was stronger in hollows than septa and the surrounding cortex in the present study. The labeling of VVA, a lectin specific for N-acetylgalactosamine, is also stronger in barrel hollows in infant animals

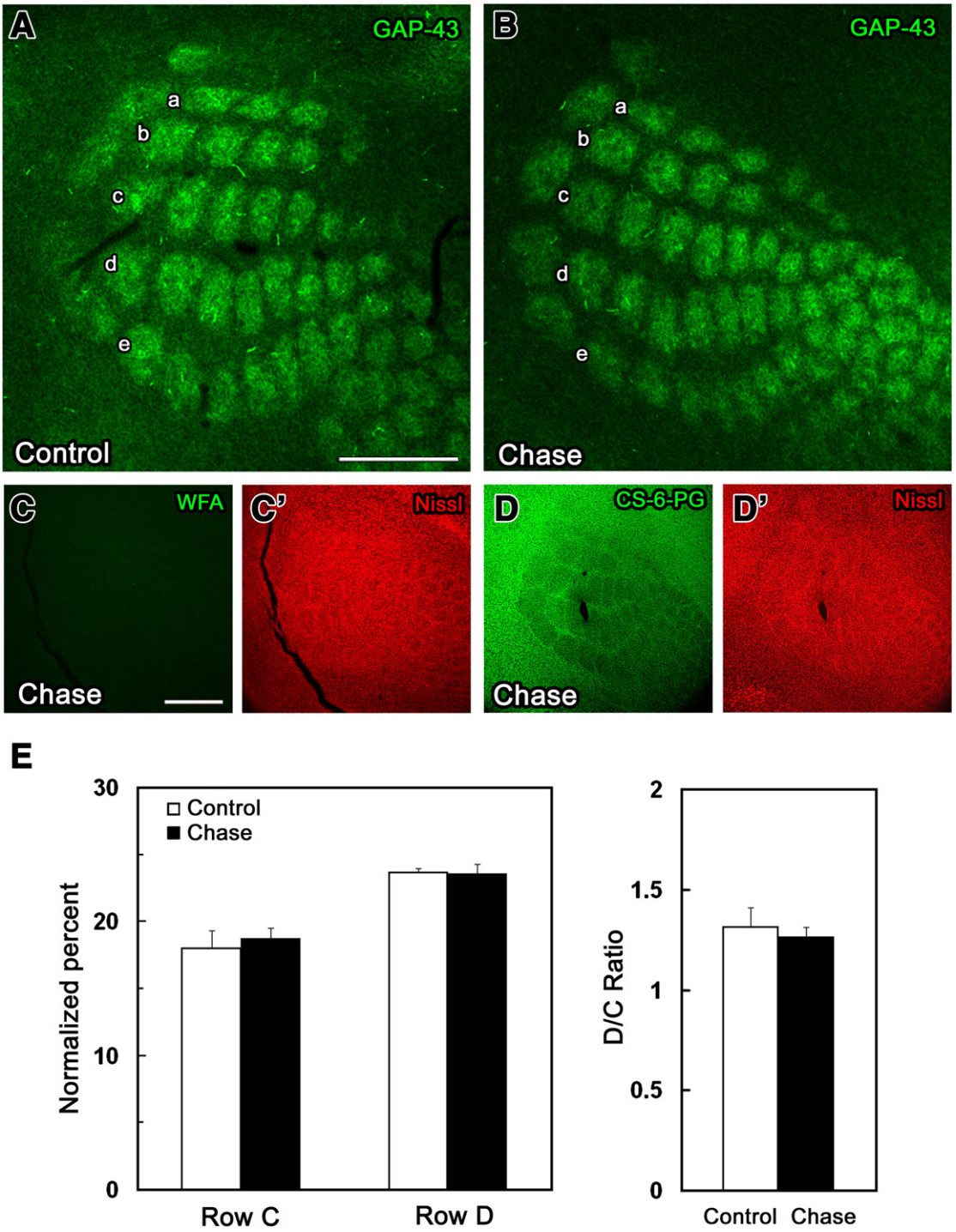

Fig. 6 – Effects of intracerebral injection of Chase on the formation of barrel structures in the PMBSF of mice. (A and B) Tangential sections showing GAP-43 immunoreactivity in the PMBSF of control and Chase-injected animals. The PMBSF was clearly visualized with the immunohistochemistry of GAP-43. (C, C′, D, and D′) Elimination of WFA labeling and immunolabeling of CS-6-PG showed degradation of CSPG GAGs in the PMBSF with Chase injection. Scale bars = 500 μm. (E) The quantitative analysis revealed that intracerebral injection of Chase did not change the normalized percent of row C and D and D/C ration.

(Bahia et al., 2008). These studies indicate the heterogeneous expression of CS GAGs in the PMBSF of early postnatal brains.

It has been shown that PNNs are frequently seen around parvalbumin-immunoreactive GABAergic interneurons in the cerebral cortex (Brückner et al., 1994; Brückner and Grosche, 2001). In the visual cortex of mammals, the number of PNNs strongly increased in all cortical layers at PN35 and reached adult levels at PN70, coincident with the end of the critical period (Lander et al., 1997; Pizzorusso et al., 2002). Rearing animals in complete darkness from birth, which is known to

Table 1

	Animal	PN10			Adult		
		Barrel		Non barrel	Barrel		Non barrel
		Hollow	Septa		Hollow	Septa	
WFA	Mouse	+	–	–	++(p)	+(p)	+(p)
	Rat	+	–	–	+(p)	++(p)	+(p)
CS-6-PG	Mouse	–	+	+	++(p)	+(p)	+(p)
	Rat	–	+	+	+(p)	++(p)	+(p)
6B4 phosphocan	Mouse	–	+	+	++(p)	+(p)	+(p)
	Rat	–	+	+	++(p)	+(p)	+(p)
3F8 Phosphocan	Mouse	–	+	+	+(p)	++(p)	+(p)
	Rat	–	+	+	+(p)	++(p)	+(p)
1G2 Neurocan	Mouse	ND			ND		
	Rat	–	+	+	–	–	–
Pab291 neurocan	Mouse	ND			ND		
	Rat	–	+	+	–	–	+(p)

(p): perineuronal nets. ND: not detected.

prolong the critical period for ocular dominance plasticity, inhibits the developmental maturation of PNNs in the visual cortex (Lander et al., 1997). The postnatal development of PNNs appears to coincide with key periods of axonal growth, synaptic refinement, myelination, and with establishment of adult-like pattern of neuronal activity (Köppe et al., 1997). More recently, it is shown that the injection of Chase into the adult visual cortex removes the CS GAGs of PNNs and thereby restores ocular dominance plasticity (Pizzorusso et al., 2002, 2006). In the present study, the spatial expression pattern of CS GAGs and CSPGs appeared after the critical period and delineated the PMBSF, however, the intracerebral injection of Chase did not influence the formation of the PMBSF pattern in mice, indicating that CS GAGs are not crucial determinants for barrel formation during development. It is shown that reduction of long term potentiation is observed in hippocampal slices pretreated with Chase (Bukalo et al., 2001). Therefore, the modulation of neuronal excitability might have a possible functional significance in CSPG expression in barrel structures.

In the PMBSF of the somatosensory cortex, the appearance of VVA labeling appears simultaneously to barrel formation in the developing rat and sensory deprivation reduced the number of VVA-labeled PNNs (Bahia et al., 2008). This observation seems to result from changes in GABAergic neurons themselves rather than changes of CSPG expression, since sensory deprivation of facial vibrissae leads to the decrease in the number of GABAergic neurons in layer IV by losing small-size interneurons (Micheva and Beaulieu, 1995). Moreover, the number and proportion of GABA-immunoreactive synaptic contacts are profoundly decreased in layer IV of PMBSF by sensory deprivation of facial vibrissae (Micheva and Beaulieu, 1995). Besides, whisker trimming did not lead to a global loss of PNNs but instead led to a specific decrease in Cat-315-positive PNNs (McRae et al., 2007). The present study further demonstrated that sensory deprivation of facial vibrissae significantly reduced the number of WFA-labeled PNNs at barrel hollows but not at barrel septa. This result indicates that afferent input from thalamic neurons promotes the maturation of GABAergic neurons in barrel hollows.

4. Experimental procedures

4.1. *Animals*

Male rats (Wistar) and mice (C57BL/6) were used for the present experiments. Animals were housed under standard conditions with a 12:12 h dark and light cycle and *ad libitum* access to commercial chow and tap water. All experimental protocols were performed in accordance with the guidelines for animal research of the Neuroscience Society of Japan to minimize the number of animals used and their suffering. To examine the effect of sensory deprivation on the density of PNNs, the mystacial pad follicles of vibrissa row C were unilaterally cauterized with an electric cauterizer (Fine Science Tools, British Columbia, Canada) on PN1 and the number of WFA-labeled PNNs was quantitatively counted in rats on PN56. To assess the effects of chondroitinase ABC on development of barrel structures, 1 μl of protease-free chondroitinase ABC (20 U/ml, Seikagaku, Tokyo, Japan) was injected intracerebrally into the PMBSF of mice on PN0, PN2, PN4, and PN6, and then animals were fixed on PN7 to immunostain with GAP-43 antibody. The elimination of CS GAGs on core proteins was confirmed by the immunoreactivity of CS-6-PG and WFA labeling.

4.2. *Antibodies and reagents*

Fluorescein isothiocyanate (FITC)-conjugated anti-mouse IgM was purchased from Pierce (Rockford, IL, USA). FITC-conjugated anti-mouse IgG and anti-rabbit IgG were purchased from Kirkegaard and Perry Laboratories (Gaithersburg, MD). Texas red Streptavidin and WFA were obtained from Vector laboratories (CA) and Sigma-Aldrich Japan (Tokyo, Japan), respectively. Red-fluorescence Nissl (NeuroTraceTM 530/615 red: N-21482) and DAPI were purchased from Invitrogen (San Diego, CA) and DOJINDO (Kumamoto, Japan). The following primary antibodies were used: CS-6-PG (mouse IgG, ICN Biomedicals), GAP-43 (mouse IgG, clone 1C6-1), GFAP (mouse IgG, Sigma-Aldrich Japan), NeuN (mouse IgG, Chemicon,

Temecula, CA), neurocan (mouse IgG, clone 1G2; Watanabe et al., 1995), neurocan (rabbit IgG, serum PAb291, Matsui et al., 1994), parvalbumin (mouse IgG, Sigma-Aldrich Japan), phosphacan (mouse IgG, clone 3F8; Developmental Studies Hybridoma Bank, Iowa, IA), and phosphacan (mouse IgM, clone 6B4, Maeda et al., 1995).

4.3. *Tissue fixation and sectioning*

Under deep anesthesia with pentobarbital (80 mg/kg), rats and mice were perfused with heparinized phosphate-buffered saline (PBS; pH 7.4) followed by 4% paraformaldehyde in 0.1 M phosphate buffer (PB, pH 7.4). Brains were removed from the skull and sectioned midsagittally into two halves. They were then postfixed overnight and flattened as described previously (Jhaveri et al., 1991). After several washes with PBS, tangential sections of flattened hemispheres were cut into 50 μm-thick sections on a vibratome (DTK-1000 microslicer, DSK, Kyoto, Japan).

4.4. *Histochemistry*

CO histochemistry was performed as described by Silverman and Tootel (1987). Briefly, PFA-fixed sections were rinsed with 10% sucrose in 0.1 M PB and then incubated for 10 min in 10% sucrose/0.05 M Tris buffer (pH 7.6) containing 275 mg/l of cobalt chloride and washed in 0.1 M PB, and incubated for 4–6 h at 40 °C in 0.1 M PB containing 0.5 g/l of 3,38-diaminobenzidine tetrahydrochloride (Sigma-Aldrich Japan), 50 g/l of sucrose, 75 mg/l of cytochrome C (type III; Sigma-Aldrich Japan), and 20 mg/l of catalase.

For immunostaining of various CSPGs, GFAP, and NeuN, standard immunofluorescence techniques were performed on the free-floating cerebral sections as described in our previous paper (Miyata et al., 2001). Briefly, the sections were pretreated with 25 mM glycine PBS for 20 min and incubated with 5% normal goat serum (NGS) in PBS containing 0.3% Triton X-100 (PBST) overnight. Then sections were incubated with the following primary antibodies in the PBST containing 5% NGS for 3 days at 4 °C: 6B4 anti-phosphacan (dilution 1:40), 3F8 anti-phosphacan (dilution 1:5), 1G2 anti-neurocan (dilution 1:10), PAb291 anti-neurocan (dilution 1:100), anti-NeuN (dilution 1:300), and anti-GFAP (dilution 1:100). The sections were then incubated with FITC-conjugated anti-mouse IgG, anti-mouse IgM, or anti-rabbit IgG (10 μg/ml) in PBST for 2 h in PBST containing red-fluorescence Nissl (dilution 1:200).

For immunostaining of CS-6-PG, the sections were treated with chondroitinase ABC to remove CS GAG chains before the immunofluorescence procedure, since anti-6′CSPG antibodies recognize CS-6-sulfated stub of core proteins disclosed after chondroitinase ABC treatment. Shortly, the sections were incubated with 0.1 unit/ml of chondroitinase ABC (Seikagaku) in 0.1 M Tris–HCl buffer (pH 8.0) containing 30 mM sodium acetate, 1 mM PMSF, 5 mM NEM, 10 μg/ml of pepstatin, and 10 μg/ml of aprotinin for 3 h at 37 °C. After several washings with PBS, the sections were incubated overnight with 5% NGS in PBST and then with 6′CSPG (dilution 1:200) in the PBST containing 5% NGS for 3 days at 4 °C. The sections were then incubated with FITC-conjugated anti-mouse IgG (10 μg/ml) for 2 h. Red-fluorescence Nissl was added at the same time as the secondary antibodies.

For labeling of WFA, the sections were pretreated with 25 mM glycine PBS for 20 min and incubated with biotinylated WFA (Sigma Aldrich Japan, 10 μg/ml) in PBST for 2 d at 4 °C. The sections were then incubated with FITC-conjugated streptavidin (10 μg/ml) for 2 h. Red-fluorescence Nissl were added at the same time as the secondary antibodies. For triple labeling, the sections were incubated with the following primary antibodies in PBST containing 5% NGS for 3 days at 4 °C: anti-phosphacan (clone 6B4; dilution 1:40), and anti-parvalbumin (dilution 1:250). The sections were then incubated with biotinylated anti-mouse IgG or IgM (7.5 μg/ml) in the PBST for 2 h followed by Texas Red Streptavidin (20 μg/ml) in the PBST for 2 h. They were incubated with biotinylated WFA (10 μg/ml) in the PBST for 2 days at 4 °C and then treated with FITC-conjugated streptavidin (10 μg/ml) and DAPI (dilution 1:1,000) in PBST for 2 h in PBST.

The sections were mounted on glass slides and sealed with Vectashield (Vector Lab). Observation was made using a LSM510 laser-scanning confocal microscope (Carl Zeiss, Germany). The sequential scanning of recording configuration for FITC was used to avoid bleed-through of FITC. Images (1024×1024) were saved as TIF files with a Zeiss LSM510 Image-Browser software and organized with Photoshop 7.0. Omission of the primary antibody did not produce any visible immunostaining on these preparations.

4.5. *Quantification*

Measurements of the entire large barrels area of mouse PMBSF and surface areas devoted to each row (C to D) were made using the software Image J. For each hemisphere, areas C and D were normalized for PMBSF area. The D/C ratio was used as a plasticity index (Schlaggar et al., 1993; Rebsam et al., 2005). The number of WFA-labeled PNNs was counted in barrel hollows and septa as described by others (Bahia et al., 2008). All values were expressed as means±SE and statistical analysis was performed by ANOVA followed by Fisher's test with α=0.05 considered as significant.

Acknowledgments

This work was supported in part by a Scientific Research Grant from the Japan Society for the Promotion of Science (No. 19500293) and the Salt Science Research Foundation (No. 0838 to S.M.). The 3F8 antibody, developed by Drs. R. K. Margolis and R. U. Margolis, was obtained from the Developmental Studies Hybridoma Bank developed under the auspices of the NICHD and maintained by the University of Iowa, Department of Biological Sciences, Iowa City, IA 52242.

REFERENCES

Bahia, C.P., Houzel, J.-C., Picanco-Diniz, C.W., Pereira, A., 2008. Spatiotemporal distribution of proteoglycans in the developing

rat's barrel field and the effects of early deafferentation. J. Comp. Neurol. 510, 145–157.
Bandtlow, C.E., Zimmermann, D.R., 2000. Proteoglycans in the developing brain: new conceptual insights for old proteins. Physiol. Rev. 80, 1267–1290.
Bradbury, E.J., Moon, L.D., Popat, R.J., King, V.R., Bennett, G.S., Patel, P.N., Fawcett, J.W., McMahon, S.B., 2002. Chondroitinase ABC promotes functional recovery after spinal cord injury. Nature 416, 636–640.
Bovolenta, P., Fernaud-Espinosa, I., 2000. Nervous system proteoglycans as modulators of neurite outgrowth. Prog. Neurobiol. 61, 113–132.
Brückner, G., Brauer, K., Härtig, W., Wolff, J.R., Rickmann, M.J., Derouiche, A., Delpech, B., Girard, N., Oertel, W.H., Reichenbach, A., 1993. Perineuronal nets provide a polyanionic, glia-associated form of microenvironment around certain neurons in many parts of the brain. Glia 8, 183–200.
Brückner, G., Seeger, G., Brauer, K., Härtig, W., Kacza, J., Bigl, V., 1994. Cortical areas are revealed by distribution patterns of proteoglycan components and parvalbumin in the Mongolian gerbil and rat. Brain Res. 658, 67–86.
Brückner, G., Bringmann, A., Härtig, W., Köppe, G., Delpech, B., Brauer, K., 1998. Acute and long-lasting changes in extracellular-matrix chondroitin-sulfate proteoglycans induced by injection of chondroitinase ABC in the adult rat brain. Exp. Brain Res. 121, 300–310.
Brückner, G., Grosche, J., Schmidt, S., Härtig, W., Margolis, R.U., Delpech, B., Seidenbecher, C.I., Czaniera, R., Schachner, M., 2000. Postnatal development of perineuronal nets in wild-type mice and in a mutant deficient in tenascin-R. J. Comp. Neurol. 428, 616–629.
Brückner, G., Grosche, J., 2001. Perineuronal nets show intrinsic patterns of extracellular matrix differentiation in organotypic slice culture. Exp. Brain Res. 137, 83–93.
Bukalo, O., Schachner, M., Dityatev, A., 2001. Modification of extracellular matrix by enzymatic removal of chondroitin sulfate and by lack of tenascin-R differentially affects several forms of synaptic plasticity in the hippocampus. Neuroscience 104, 359–369.
Cases, O., Vitalis, T., Seif, I., De Maeyer, E., Sotelo, C., Gaspar, P., 1996. Lack of barrels in the somatosensory cortex of monoamine oxidase A-deficient mice, role of a serotonin excess during the critical period. Neuron 16, 297–307.
Celio, M.R., Blümcke, I., 1994. Perineuronal nets-a specialized form of extracellular matrix in the adult nervous system. Brain Res. Rev. 19, 128–145.
Celio, M.R., Spreafico, R., De Bias, S., Vitellaro-Zuccarello, L., 1998. Perineuronal nets, past and present. Trends Neurosci. 21, 510–515.
Cooper, N.G.F., Steindler, D.A., 1986. Lectins demarcate the barrel subfield in the somatosensory cortex of the early postnatal mouse. J. Comp. Neurol. 249, 157–169.
Corvett, L., Rossi, F., 2005. Degradation of chondroitin sulfate proteoglycans induces sprouting of intact Purkinje axons in the cerebellum of the adult rat. J. Neurosci. 25, 7150–7158.
Cybulska-Klosowicz, A., Zakrzewska, R., Pyza, E., Kossut, M., Schachner, M., 2004. Reduced plasticity of cortical whisker representation in adult tenascin-C-deficient mice after vibrissectomy. Eur. J. Neurosci. 20, 1538–1544.
Eng, L.F., Chirnikar, R.S., Lee, Y.L., 2000. Glial fibrillary acidic protein: GFAP-thirty-one years (1969–2000). Neurochem. Res. 25, 1439–1451.
Fox, K., 1992. A critical period for experience-dependent synaptic plasticity in rat barrel cortex. J. Neurosci. 12, 826–1836.
Frostig, R.D., 2006. Functional organization and plasticity in the adult rat barrel cortex, move out-of-the-box. Curr. Opin. Neurobiol. 16, 445–450.
Fukuichi-Shimogori, T., Grove, E.A., 2001. Neocortex patterning by the secreted signaling molecule FGF8. Science 294, 1071–1074.
Furuta, A., Rothstein, J.D., Martin, L.J., 1997. Glutamate transporter protein subtypes are expressed differentially during rat CNS development. J. Neurosci. 17, 8363–8375.
Galtrey, C.M., Fawcett, J.W., 2007. The role of chondroitin sulfate proteoglycans in regeneration and plasticity in the central nervous system. Brain Res. Rev. 85, 2813–2823.
Hannan, A.J., Blakemore, C., Katsnelson, A., Vitalis, T., Huber, K.M., Bear, M., Roder, J., Kim, D., Shin, H.S., Kind, P.C., 2001. PLC-beta1, activated via mGluRs mediates activity-dependent differentiation in cerebral cortex. Nat. Neurosci. 4, 282–288.
Härtig, W., Brauer, K., Brückner, G., 1992. *Wisteria floribunda* agglutininlabeled nets surround parvalbumin-containing neurons. NeuroReport 3, 869–872.
Iwasato, T., Datwani, A., Wolf, A.M., Nishiyama, H., Taguchi, Y., Tonegawa, S., Knopfel, T., Erzurumlu, R.S., Itohara, S., 2000. Cortex-restricted disruption of NMDAR1 impairs neuronal patterns in the barrel cortex. Nature 406, 726–731.
Jhaveri, S., Erzurumlu, R.S., Crossin, K., 1991. Barrel construction in rodent neocortex, role of thalamic afferents versus extracellular matrix molecules. Proc. Natl. Acad. Sci. U. S. A. 88, 4489–4493.
John, N., Krügel, H., Frischknecht, R., Smalla, K.-H., Schultz, C., Kreutz, M.R., Gundelfinger, E.D., Seidenbecher, C.I., 2006. Brevican-containing perineuronal nets of extracellular matrix in dissociated hippocampal primary cultures. Mol. Cell. Neurosci. 31, 774–784.
Katoh-Senba, R., Matsuda, M., Kato, K., Oohira, A., 1995. Chondroitin sulphate proteoglycans in the rat brain, candidates for axon barriers of sensory neurons and the possible modification by laminin of their actions. Eur. J. Neurosci. 7, 613–621.
Köppe, G., Brückner, G., Brauer, K., Härtig, W., Bigl, V., 1997. Developmental patterns of proteoglycan-containing extracellular matrix in perineuronal nets and neuropile of the postnatal rat brain. Cell Tissue Res. 288, 33–41.
Lander, C., Kind, P., Maleski, M., Höckfield, S., 1997. A family of activity-dependent neuronal cell-surface chondroitin sulfateproteoglycans in cat visual cortex. J. Neurosci. 17, 1928–1939.
Lin, C.-S., Lu, S.M., Schmechel, D.E., 1985. Glutamic acid decarboxylase immunoreactivity in layer IV of barrel cortex of rat and mouse. J. Neurosci. 5, 1934–1939.
Maeda, N., Hamanaka, H., Oohita, A., Noda, M., 1995. Purification, characterization and developmental expression of a brain-specific chondroitin sulfate proteoglycan, 6B4 proteoglycan/phosphacan. Neuroscience 67, 23–35.
Matsui, F., Watanabe, E., Oohira, A., 1994. Immunological identification of two proteoglycan fragments derived from neurocan, a brain-specific chondroitin sulfate proteoglycan. Neurochem. Int. 25, 425–431.
McRae, P.A., Rocco, M.M., Kelly, G., Brumberg, J.C., Matthews, R.T., 2007. Sensory deprivation alters aggrecan and perineuronal net expression in the mouse barrel cortex. J. Neurosci. 27, 5405–5413.
Micheva, K.D., Beaulieu, C., 1995. An anatomical substrate for experience-dependent plasticity of the rat barrel field cortex. Proc. Natl. Acad. Sci. U. S. A. 92, 11834–11838.
Mitrovic, N., Mohajeri, H., Schachner, M., 1996. Effects of NMDA receptor blockage in the developing rat somatosensory cortex on the expression of the glia-derived extracellular matrix glycoprotein tenascin-C. Eur. J. Neurosci. 8, 1793–1802.
Miyata, S., Takamatsu, S., Maekawa, S., Matsumoto, K., Watanabe, K., Kiyohara, T., Hatton, G.I., 2001. Plasticity of

neurohypophysial terminals with increased hormonal release during dehydration: ultrastructural and biochemical analyses. J. Comp. Neurol. 343, 413–427.
Miyata, S., Nishimura, Y., Hayashi, N., Oohira, A., 2005. Construction of perineuronal net-like structure by cortical neurons in culture. Neuroscience 136 , 95–104.
Miyata, S., Nishimura, Y., Nakashima, T., 2007. Perineuronal nets protect against amyloid β-protein neurotoxicity in cultured cortical neurons. Brain Res. 1150, 200–206.
Oohira, A., Matsui, F., Katoh-Senba, R., 1991. Inhibitory effects of brain chondroitin sulfate proteoglycans on neurite outgrowth from PC12D cells. J. Neurosci. 11, 822–827.
Peterson, C.C.H., 2007. The functional organization of the barrel cortex. Neuron 56, 339–355.
Pizzorusso, T., Medini, P., Berardi, N., Chierzi, S., Fawcett, J.W., Maffei, L., 2002. Reactivation of ocular dominance plasticity in the adult visual cortex. Science 898, 1248–1251.
Pizzorusso, T., Medini, P., Landi, S., Baldini, A., Berardi, N., Maffei, L., 2006. Structural and functional recovery from early monocular deprivation in adult rats. Proc. Natl. Acad. Sci. U. S. A. 103, 8517–8522.
Rebsam, A., Seif, I., Gaspar, P., 2005. Dissociating barrel development and lesion-induced plasticity in the mouse somatosensory cortex. J. Neurosci. 19, 706–710.
Schlaggar, B.L., Fox, K., O, Leary, D.D.M., 1993. Postsynaptic control of plasticity in developing somatosensory cortex. Nature 364, 623–626.
Silverman, M.S., Tootel, R.B., 1987. Modified technique for cytochrome oxidase histochemistry, increased staining intensity and compatibility with 2-deoxyglucose autoradiography. J. Neurosci. Methods 19, 1–10.
Steindler, D.A., Settles, D., Erickson, H.P., Laywell, E.D., Yoshiki, A., Faissner, A., Kusakabe, M., 1995. Tenascin knockout mice, barrels, boundary molecules, and glial scars. J. Neurosci. 15, 1971–1983.
Van der Loos, H., Woolsey, T.A., 1973. Somatosensory cortex, structural alterations following early injury to sense organs. Science 179, 395–398.
Voutsinos-Porche, B., Knott, G., Tanaka, K., Quairiaux, C., Welker, E., Bonento, G., 2003. Glial glutamate transporters and maturation of the mouse somatosensory cortex. Cereb. Cortex 13, 1110–1121.
Watanabe, E., Aono, S., Matsui, F., Yamada, Y., Naruse, I., Oohira, A., 1995. Distribution of a brain-specific proteoglycan, neurocan, and the corresponding mRNA during the formation of barrels in the rat somatosensory cortex. Eur. J. Neuorsci. 7, 547–554.
Welker, E., Armstrong-James, M., Bronchti, G., Ourednik, W., Gheorghita-Baechler, F., Dubois, R., Guernsey, D.L., Van der Loos, H., Neumann, P.E., 1996. Altered sensory processing in the somatosensory cortex of the mouse mutant barrelless. Science 271, 1864–1867.
Wong-Riley, M.T., Welt, C., 1980. Histochemical changes in cytochrome oxidase of cortical barrels after vibrissal removal in neonatal and adult mice. Proc. Natl. Acad. Sci. U. S. A. 77, 2333–2337.
Woolsey, T.A., Van der Loos, H., 1970. The structural organization of layer IV in the somatosensory region (SI) of mouse cerebral cortex. The description of a cortical field composed of discrete cytoarchitectonic units. Brain Res. 17, 205–242.
Woolsey, T.A., Wann, J., 1976. Area changes in mouse cortical barrels following vibrissal damage at different postnatal ages. J. Comp. Neurol. 170, 53–66.
Yamaguchi, Y., 2000. Lecticans, organizers of the brain extracellular matrix. Cell. Mol. Life Sci. 57, 276–289.